Simulation of Idle Running Operating Characteristics for Low-Power Asynchronous Motors

Raluca-Cristina (Presură) Nicolae
University of Craiova, Faculty of Electrical Engineering, Craiova, Romania
raluca.presura92@gmail.com, nmarianstefan@yahoo.com

***Abstract* - The opportunity of this work is backed by the possibility to predetermine the operating characteristics of an asynchronous motor in idle running. This contributes to the realization of a high performance electric drive. An analysis is aimed for low power asynchronous motors used in different types of applications, such as robots, medical equipment and home appliances, transportation systems a.s.o. It is insisted on an advanced mathematical model that provides the best results in simulations and applications [1]. The simulations are important for their quality and precision because they allow us to anticipate the motor behavior and also to establish the errors between the simulation and experimental results. The mathematical model used considered the equations written in the two-axes theory, the rotor quantities being expressed in the fixed stator reference frame. The need for knowledge of qualitative and quantitative dynamic behavior related to the field of use determined major investments and extensive research in large laboratories. Research on an asynchronous motor with a power of 1.1 kW with variable parameters proved that, between the idle running simulated and experimentally determined values, the errors do not exceed 3.97%. These results authorize the conducted research, providing qualitative and quantitative correct simulations for the rated regime.**

Cuvinte cheie: *motoare asincrone de puteri mici, modelare, simulare, regimuri dinamice si stationare.*

Keywords: *low-power asynchronous motors, modeling, simulation, stationary and dynamic regimes.*

I. INTRODUCTION

From the economic perspective, the asynchronous motor must possess a low manufacturing cost and, at the same time, a lower operating cost. In such circumstances, the asynchronous motor is loaded both mechanically and electrically. For a proper operation, information about the evolution of the quantities specific to a given regime should be known.

For low power motors, the direct loading method is used mostly, and it involves coupling the test motor with another electric machine as a load, e.g. a dc generator or, in case of a low power operation, a magnetic power brake, changing the load within the $(0 \div 1.2)P_{2N}$ limits.

The method is precise and practical in terms of obtaining the necessary data. It has disadvantages due to the need for a more complex loading and measurement equipment, and also due to the large energy consumption.

The repeated and multiple simulations presented highlight that the design [1-10], is optimal for a motor operating under rated conditions. The operating characteristics correspond to the requirements of the beneficiary, with minimal running costs (conditioned by high values obtained for the efficiency and power factor).

Simulations based on a complex mathematical model are difficult to perform, but this complexity can still be solved using advanced numerical computation methods.

II. THE MATHEMATICAL MODEL OF THE ASYNCHRONOUS MOTOR

The quality of the obtained simulations depends on the mathematical model used, which must take into account the basic electromagnetic phenomena occuring in the machine.

The correctness of these simulations allows us to state that the errors occuring between the measured and simulated values are compliant with the limits accepted by the standards.

The precise mathematical models used requires considering the influence of magnetic saturation and the current repression on the parameters of the machine [11-21].

For the simulations was used a mathematical model with equations written in the two axes theory, with the rotor quantities in the fixed stator reference frame (ω_B=0),

$$\frac{di_{ds}}{dt} = \frac{1}{L_s L_r' - L_{sh}^2}\left[\begin{array}{l} - R_s L'_r\, i_{ds} + \omega L_{sh}^2 i_{qs} + \\ + R'_r\, L_{sh} i'_{dr} + \omega L'_r\, L_{sh} i'_{qr} + L'_r\, u_{ds} + 0 \end{array}\right]$$

$$\frac{di_{qs}}{dt} = \frac{1}{L_s L_r' - L_{sh}^2}\cdot\left[\begin{array}{l} - \omega L_{sh}^2 i_{ds} - R_s L'_r\, i_{qs} - \\ - \omega L'_r\, L_{sh} i'_{dr} + R'_r\, L_{sh} i'_{qr} + 0 + L'_r\, u_{qs} + 0 \end{array}\right]$$

$$\frac{di'_{dr}}{dt} = \frac{1}{L_s L_r' - L_{sh}^2}\left[\begin{array}{l} R_s L_{sh} i_{ds} - \omega L_s L_{sh} i_{qs} - \\ - R'_r\, L_s i'_{dr} - \omega L_s L'_r\, i'_{qr} - L_{sh} u_{ds} + 0 \end{array}\right] \quad (1)$$

$$\frac{di'_{qr}}{dt} = \frac{1}{L_s L_r' - L_{sh}^2}\left[\begin{array}{l} \omega L_s L_{sh} i_{ds} + R_s L_{sh} i_{qs} + \\ + \omega L_s L'_r\, i'_{dr} - R'_r\, L_s i'_{qr} + 0 - L_{sh} u_{qs} \end{array}\right]$$

To these is added the equation of motion:

$$\frac{d\omega}{dt} = \frac{p}{J}\left[\frac{3}{2} p L_{sh}(i_{qs} i'_{dr} - i_{ds} i'_{qr}) - m_r\right], \quad (2)$$

where the square brackets mark the electromagnetic torque:

$$m = \frac{3}{2} p L_{sh}(i_{qs} i'_{dr} - i_{ds} i'_{qr}). \quad (3)$$

A.Resuls Obtained Through Simulation

The theoretical and experimental researches were carried out for a squirrel cage asynchronous motor with the following rated values: P_N=*1.1* kW - rated power; U_N=*400* V – rated voltage; I_{1N}=*2.997* A – rated current; n_1=*1500* rot/min – synchronous speed; M_N=8.043 Nm – rated torque; s_N=*8.7*% - rated slip and the electric parameters R_s=5.366 Ω, R'_r= 6.836 Ω, $L_{s\sigma}$=0.028 H, $L'_{r\sigma}$=0.018 H, L_{sh}=0.412 H, J=0.00224 kg·m^2.

The operating characteristics are: cosφ=0.82; η=0.78; M_N=8.043 Nm; M_{max}=2.3·M_N; M_p=1.64·M_N; I_p=5.75·I_N.

B.Start-up Dynamic Regime in Idle Running

The numerical solving has been performed with the fourth order Runge-Kutta method of the previously presented mathematical model. After each step results a new value of „ω –the rotor angular speed", and some other quantities of interest. With respect to this variable, the program sets the following variable parameters of the motor: $R_2(\omega)$– the resistance of a rotor phase, $L_1(\omega)$, $L_2(\omega)$- the leakage inductances for a stator / rotor phase, $L_h(\omega)$ – the main inductance. These parameters are dependent on the current repression in the rotor bar and on the magnetic saturation, so they depend on the rotor speed.

We may state that the mathematical model is nonlinear as it has variable parameters, and the variation plots of the parameters are provided in tables in the solving program.

The simulations conducted and presented further take into account the following aspects:

- the connection to the power supply network of the asynchronous motor which trains a mechanism characterized by a very small electromagnetic torque M_{st}=0.04*M_N=0.322 N·m and a very high moment of inertia J_2=40*J=0.0896 kgm^2, for t= (0 ÷ 1.5) s;

- at the operation in iddle running, the mechanism is decoupled (M_{st}=0.02*M_N=0.161 N·m and J_2=1*J=0.00224 kg·m^2) and the supply voltage it reduces to zero, t= (1.5 ÷ 4.0) s.

When the rated speed is reached, Fig. 1.d, the torque and the current are decreased, reaching low values corresponding to the operation in idle running. The variation curves for the current, torque and speed in this interval may be noticed in Fig. 1.

During the analyzed dynamic regime, due to the magnetic saturation, the useful flux and the main inductance change, the plots for the relationship between these quantities and the magnetic saturation being provided in Fig. 2 and Fig. 3.

The analysis of Fig. 1 proves that, in the first moments, the currents and the torque have high values, quickly accelerating the rotor.

The large duration of the dynamic regime allows, for each period of the voltage waveform, the computation of the average (or rms) values for M- the torque, I_{10} –the current, S_{10}, P_{10}, Q_{10} –the apparent, active, reactive powers received from the network, P_{c0} –the power corresponding to the rotor acceleration, cosφ_{10} –the power factor and to study their variation plots, as in Fig.4. In Fig.4.a may be easily noticed the two stages of the dynamic regime: t= (0 ÷ 1.5) s – the connection to the three-phase supply network and t= (1.5 ÷ 4.0) the linear decrease of the voltage until the motor is disconnected.

In Fig.4.b is simulated a current curve (rms value) for the whole dynamic regime. When the motor is supplied, a large current may be noticed, I_p=13.2 A, rapidly decreasing to the idle running value I_{10}=1.593 A, and linearly decreasing to zero with the voltage. Similarly, the variation curves of the torque *M* (Fig.4.c), S_{10}, P_{10}, Q_{10} – the apparent, active and reactive powers (Fig.4.d, Fig.4.e, Fig.4.f) may be noticed.

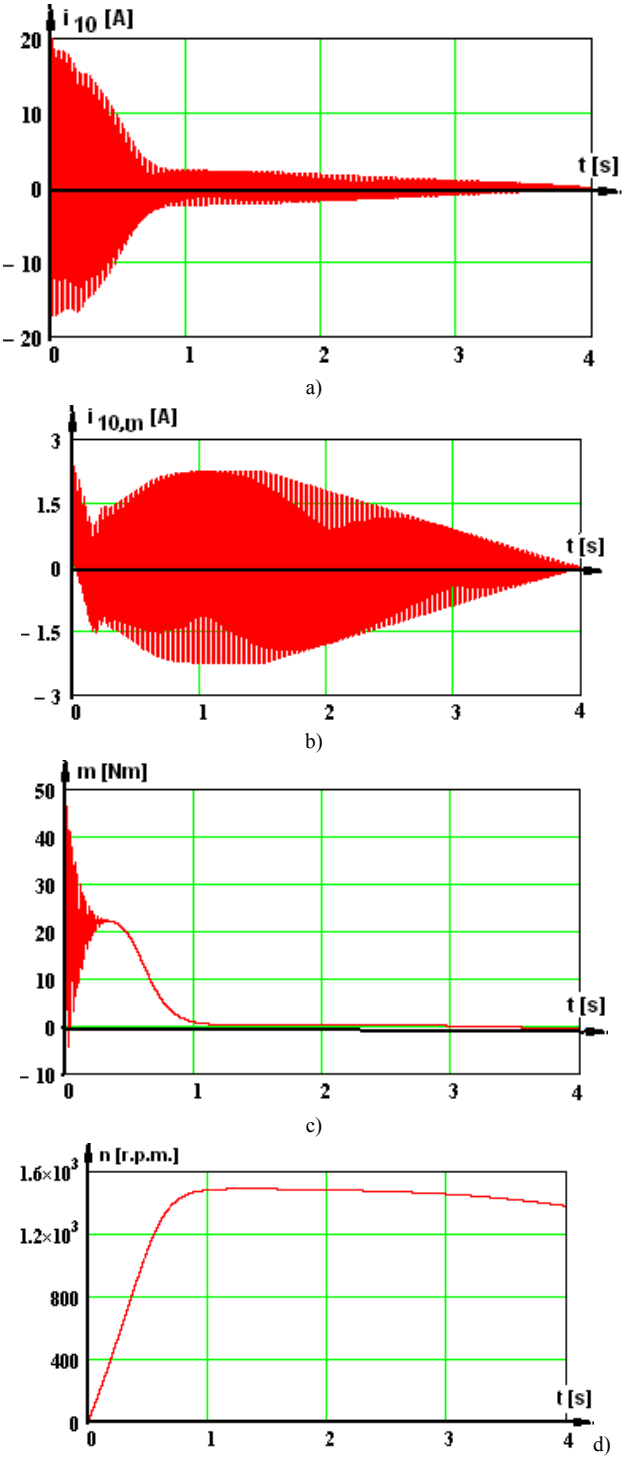

Fig.1. The variation plots for the idle running rotor start and for the coupling of a load with a large moment of inertia for: a) current, b) magnetizing current, c) electromagnetic torque, d) rotor speed.

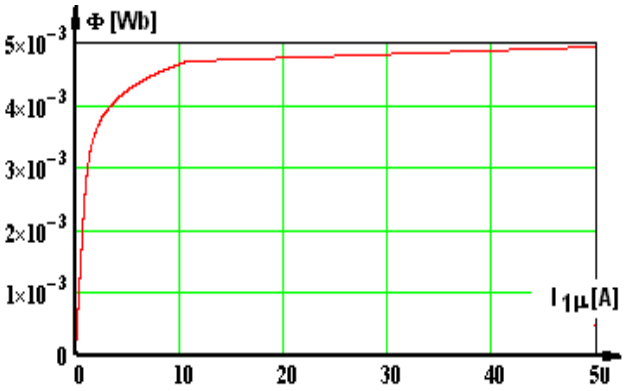

Fig.2. The magnetization curve of the analyzed motor.

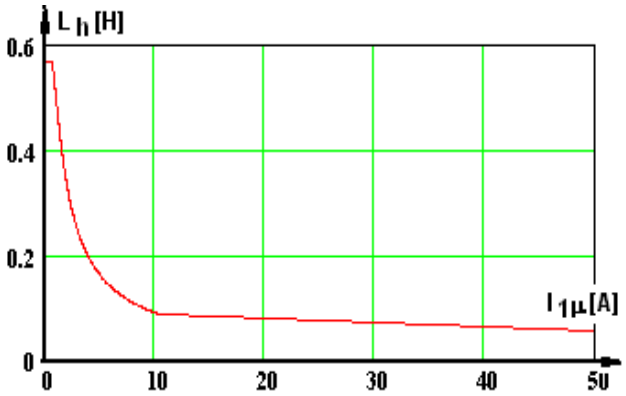

Fig.3. The variation curve of the main inductance with the magnetic saturation ($I_{1\mu}$ –the magnetizing current).

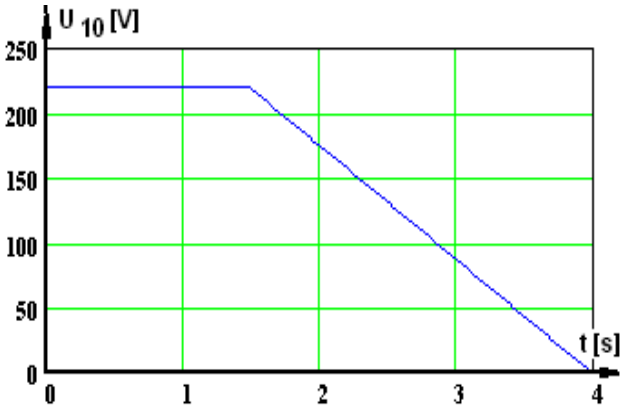

a)

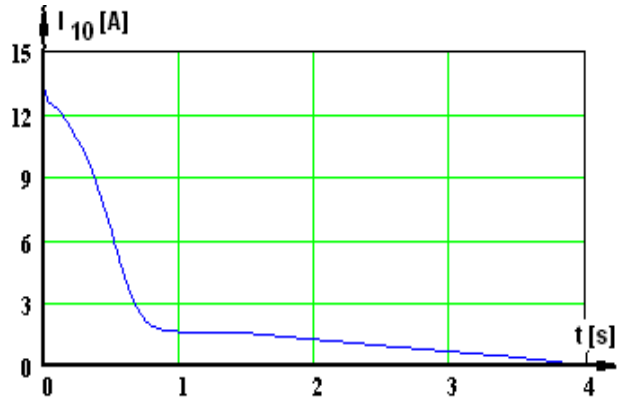

b)

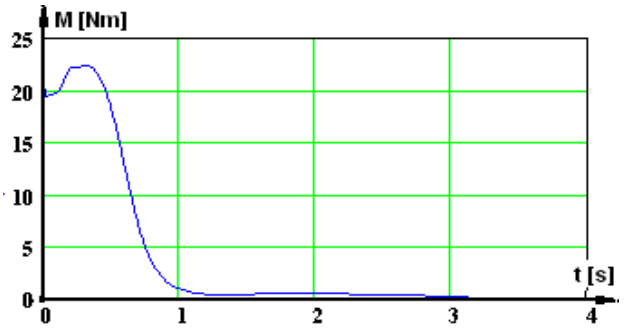

c)

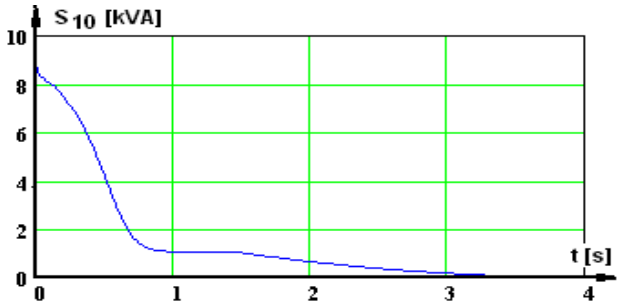

d)

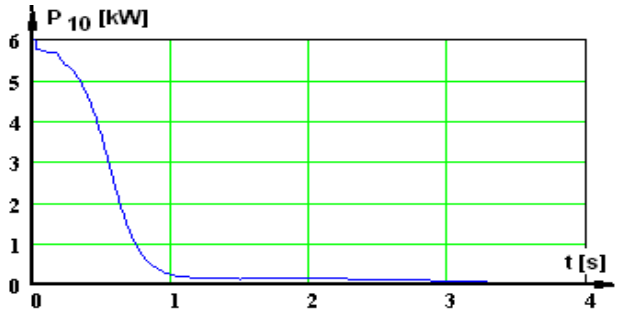

e)

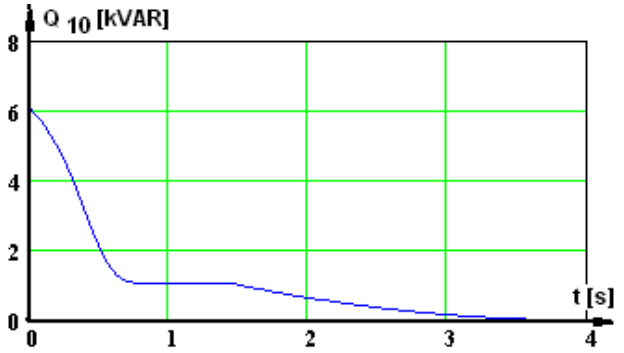

f)

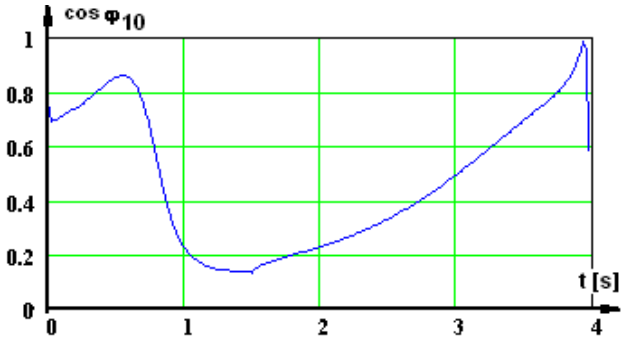

g)

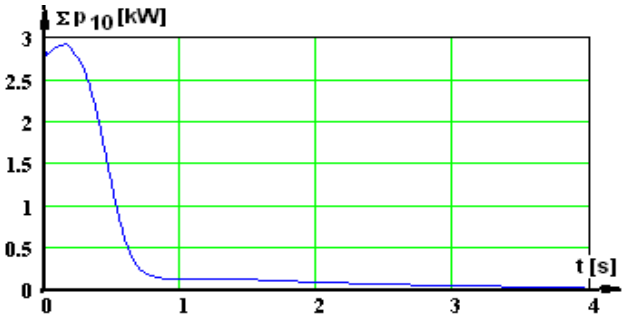

i)

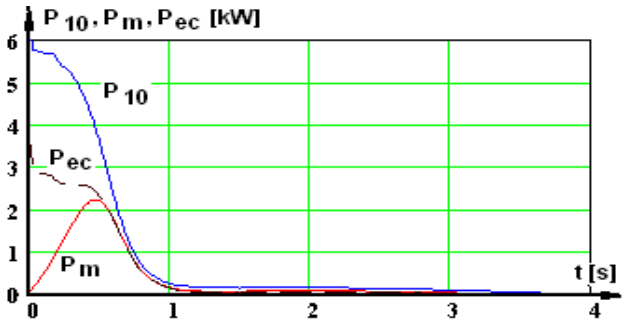

j)

Fig.4. The variation plots for the average (rms) values of the analyzed dynamic regime for: a) voltage, b) current, c) electromagnetic torque, d) apparent power, e) active power, f) reactive power, g) power factor, i) total losses, j) P_{10} - active power received from the network, P_m – electromagnetic power, P_{ec} –power corresponding to the rotor acceleration.

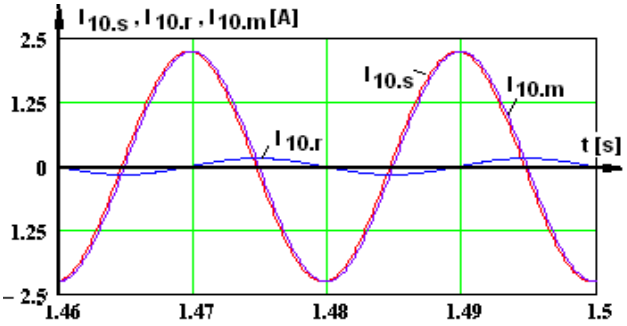

Fig.5. The current variation curves for the stable idle running operation: $I_{10.s}$- stator current, $I_{10.r}$-rotor current, $I_{10.m}$ –magnetizing current.

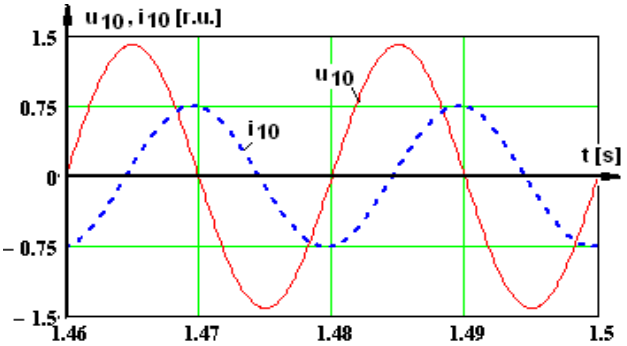

Fig.6. The variation plots in per unit values for the motor operating in idle running for: u_{10}, i_{10} –the phase voltage and current.

An interesting plot may be observed for the simulated power factor Fig.4.g, and for the total losses in Fig.4.i, respectively. For the motor in idle running from Fig. 5, the simulation results are presented for i_s, i_r, i_m –the phase stator, rotor and magnetization currents, respectively. In Figure6 are depicted the per unit stator voltage and current of a stator phase, and a large phase shift $\varphi_{10}=84^o$ is present.

By eliminating the time „*t*" variable –from the simulations depicted in Fig.6, the operating plots of the motor in idle running result:

- the current plot, $I_{10}=f(U_{10})$,
- the plots for the powers received from the network, $P_{10}=f(U_{10})$ –active, $S_{10}=f(U_{10})$ –apparent, $Q_{10}=f(U_{10})$ – reactive;
- the speed plot, $n_0=f(U_{10})$;
- the power factor plot, $\cos\varphi_{10}= f(U_{10})$.

All of these plots are depicted in Fig. 7, Fig. 8,...,Fig. 13, where the simulation results are compared with the experimental data from a test stand.

III. Simulations and Experimental Tests

The experimental data [22-25], were collected for establishing the operating plots of the squirell cage asynchronous motor in idle running with the rated parameters: P_N=1.1 kW, U_N=400 V, I_{1N}=2.997 A, n_1=1500 rpm. at the „Electrical Machines Laboratory" of the Faculty.

A.The Idle Running Performances

The three-phase squirell cage asynchronous motor was supplied with a variable voltage U_{10}=(0 -4000) V and, with a three-phase digital multimeter were measured:

I_{10} I_{20}, I_{30} – the currents of the three phases,

U_{10} U_{20}, U_{30},-the phase voltages;

S_{10}, P_{10}, Q_{10} –the apparent, active and reactive powers,

$\cos\varphi_{10}$– the power factor and *n*– the speed, respectively, with an electronic tachometer.

The performances for the idle running operation are depicted in Fig.7, Fig.8,...,Fig.13.

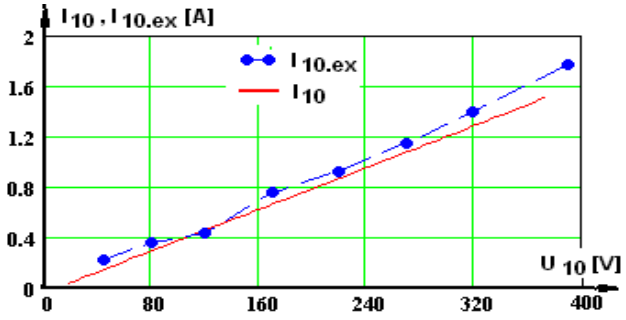

Fig.7. The variation plots for the currents at the motor operating in idle running: I_{10} -simulated and $I_{10.ex}$ -experimental.

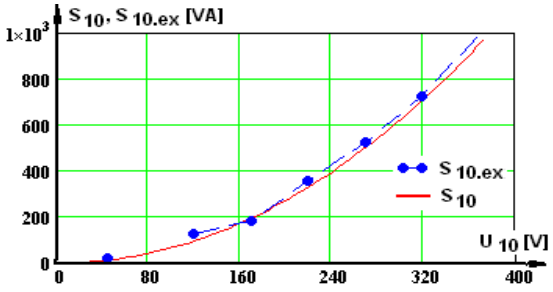

Fig.8. The evolution of the apparent powers for the idle running operation: S_{10} –simulated and $S_{10.ex}$ -experimental.

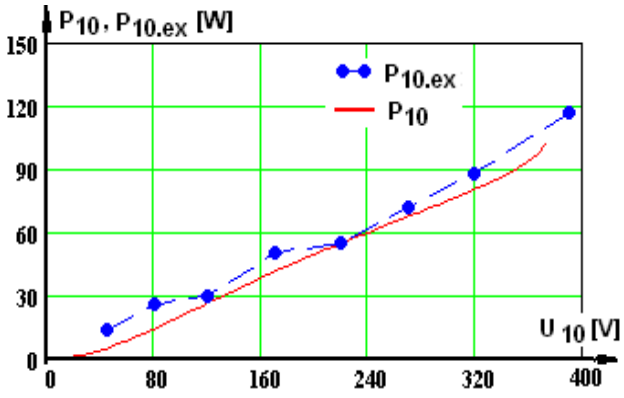

Fig.9. The evolution of the active powers for the idle running operation: P_{10} -simulated and $P_{10.ex}$ -experimental.

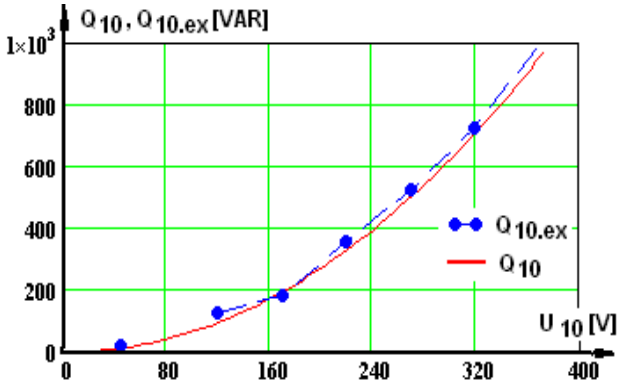

Fig.10. The evolution of the reactive powers for the idle running operation: Q_{10} -simulated and $Q_{10.ex}$ -experimental.

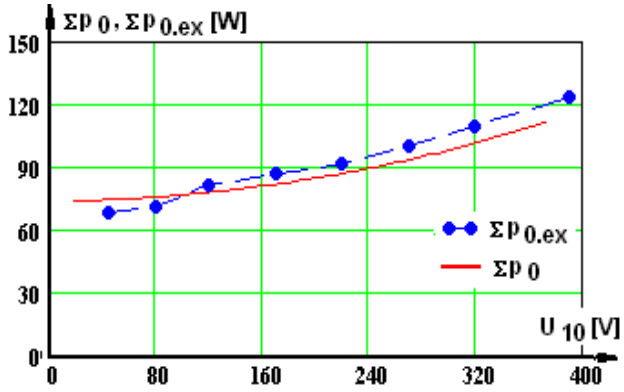

Fig.11. The variation curves for the total losses of the motor operating in idle running: Σp_0 -simulated and $\Sigma p_{0.ex}$ -experimental.

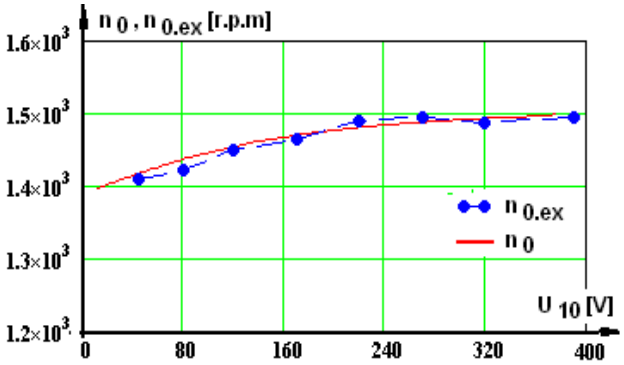

Fig.12. The speed variation curves in idle running: n_0 -simulated and $n_{0.ex}$ -experimental.

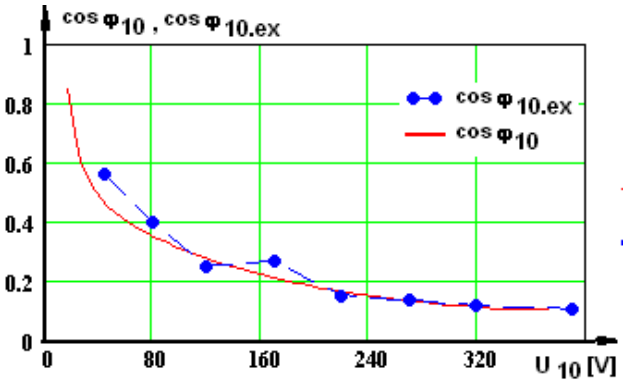

Fig.13. The variation curves for the power factor of the motor operating in idle running: $\cos\varphi_{10}$ -simulated and $\cos\varphi_{10.ex}$ -experimental.

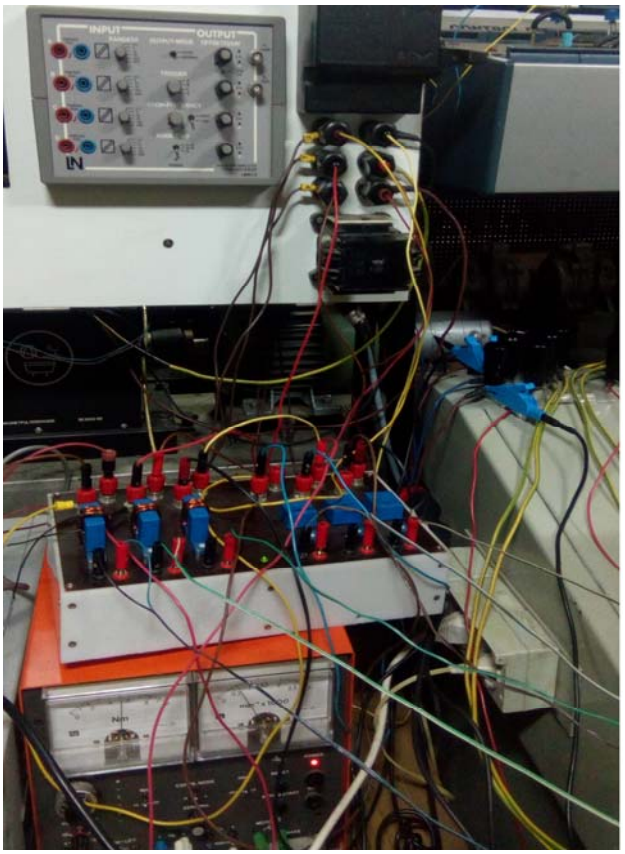

a)

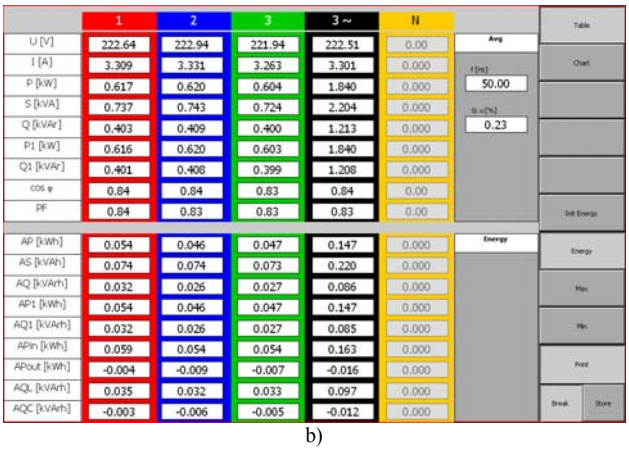

	1	2	3	3 ~	N
U [V]	222.64	222.94	221.94	222.51	0.00
I [A]	3.309	3.331	3.263	3.301	0.000
P [kW]	0.617	0.620	0.604	1.840	0.000
S [kVA]	0.737	0.743	0.724	2.204	0.000
Q [kVAr]	0.403	0.409	0.400	1.213	0.000
P1 [kW]	0.616	0.620	0.603	1.840	0.000
Q1 [kVAr]	0.401	0.408	0.399	1.208	0.000
cos φ	0.84	0.84	0.83	0.84	0.00
PF	0.84	0.83	0.83	0.83	0.00
AP [kWh]	0.054	0.046	0.047	0.147	0.000
AS [kVAh]	0.074	0.074	0.073	0.220	0.000
AQ [kVArh]	0.032	0.026	0.027	0.086	0.000
AP1 [kWh]	0.054	0.046	0.047	0.147	0.000
AQ1 [kVArh]	0.032	0.026	0.027	0.085	0.000
APin [kWh]	0.059	0.054	0.054	0.163	0.000
APout [kWh]	-0.004	-0.009	-0.007	-0.016	0.000
AQL [kVArh]	0.035	0.032	0.033	0.097	0.000
AQC [kVArh]	-0.003	-0.006	-0.005	-0.012	0.000

b)

Fig. 14. Experimental tests: the test bench, the module with transducers and the data acquisition system; b) experimental data.

For the rated voltage U_{1N}=380 V, the simulation and experimental results are depicted in Tab. I.

TABLE I

RESULTS: IDLE RUNNING PERFORMANCES

Quantity analyzed	Symbol	MU	Results for the idle running operation		
			Simulated	Experimental	Error
Supply voltage	U_{10}	V	380	380	-
Phase stator current	I_{10}	A	1.593	1.612	1.19%
Speed	n_0	r/min	1498	1495	0.205%
Active power received from the supply network	P_{10}	W	109	113	3.67%
Apparent power received	S_{10}	VA	998	1030	3.21%
Reactive power received from the supply network	Q_{10}	VAR	994	1020	2.62%
Power factor	$\cos\varphi_{10}$		0.122	0.124	1.64%
Losses in the stator winding	p_{Cu10}	W	37.2	38.4	3.23%
Losses in the rotor winding	p_{Cu20}	W	0.0031	0.0029	4.6%

CONCLUSIONS

The analysis of Tab. I provest that, for a motor operating in idle running, the deviations between the calculated values and those determined experimentally are very small, below 3.97%.

The results confirm the quality of the conducted research, proving that simulations can be conducted for other types of motors, in order to check if they correspond to the exploitation requirements.

In the design process of the actual asynchronous motors, the simulation of the operating characteristics must be a mandatory stage.

On this basis, the electromagnetic stresses and constructive solutions can be definitively fixed, so that the machine corresponds to the the exploitation requirements.

ACKNOWLEDGMENT

This paper was realized under the frame of the grant POC 59/05.09.2016, ID: P_40_401, SMIS 106021.

Contribution of authors:

First author – 100%

Received on August 05, 2018

Editorial Approval on November 15, 2018

REFERENCES

[1] A. Boglietti, A. Cavagnino, et al., "International standards for the induction motor efficiency determination: A critical analysis of the stray load loss determination", IEEE-IAS Trans. on Ind. Appl. 40, 2004, no. 5, p.1294-1301.

[2] A. Campeanu., I. Vlad, Complements of electrical machines dynamics. Tests and theory summary. Universitaria Publishing House, Craiova, 2007 (in Romanian).

[3] Fu W. N., Ho S. L., and Wong H. C., Design and analysis of practical induction motors, IEEE Trans. on Magnetics, vol. 37, no. 5, pp. 3663-3667, 2001.

[4] CEI 60034-2-1 Standard: "Rotating electrical machines-Part 2-1. Standard methods for determining losses and efficiency from tests", Edition 1.0 2007

[5] I. Vlad, A. Campeanu, S. Enache, M.A. Enache, Dynamic State of Low Power Asynchronous Motors in Direct-on-Line Starting, Annals of the University of Craiova, Electrical Engineering Series, No. 41, 2017; ISSN 1842-4805, pp. 54-59.

[6] C. Nica, and M.A. Enache, "About Operation Characteristics of Lowe Power Synchronous Motors at Frequency Command", International Symposium on Power Electronics, Electrical Drive, Automation and Motion Ischia, Italy, JUN 11-13, 2008.

[7] A. Kelemen, M. Imecs, Regulation systems with orientation by field of alternationg current machines. Academy Publishing House, Bucharest, 1989 (in Romanian).

[8] A. Kelemen, M. Imecs, Vector Control of Induction Machines Drives, OMIKK, Budapest, 1992.

[9] P. Kovacs, Analysis of transient states of electrical machines, Technical Publishing House, Bucharest, 1980 (in Romanian).

[10] S. Enache, I. Vlad, "Program for Study of Electrical Machines Dynamic Regimes", in Proceedings of The International Conference on Applied and Theoretical Electrotechnics, Craiova, June 4 6, 1998.

[11] A. Campeanu, I. Cautil, I. Vlad, S. Enache, Modelling and simulation of alternating current machines. Romanian Academy Publishing House, Bucharest, 2012 (in Romanian).

[12] S. Curteanu, Numerical computation and symbols in MATHCAD, Matrix Rom Publishing House, Bucharest, 2004 (in Romanian).

[13] A. Fasquelle, D. Saury, S. Harmand, and A. Randria, "Numerical study of convective heat transfer in end region of enclosed induction motor of railway traction," IJEET International Journal of Electrical Engineering in Transportation, Dec. 2006.

[14] Khezzar A., Kaikaa M., Boucherma M., Analytical Investigation of Rotor Slot Harmonics in a Three Phase Induction Motor with Broken Rotor Bars, EPE 2005, Dersden, 11-14 Septemper, CD Proceeding.

[15] R.D. Lorentz, "Future Motor Drive Technology Issues and their Evolution", 12th Int. Power Electronics and Motion Conf. (EPE-PEMC), Portoroz, Slovenia, 2006, CD-ROM.

[16] St. Maksay, D. Stoica, Matematici asistate de calculator, Editura Politehnica Timisoara, 2006

[17] D. Samarkanov, F. Gillon, P. Brochet, D. Laloy, "Techno-economic Optimization of Induction Machines: an Industrial Application", ACEMP - Electromotion 2011, Istanbul –Turkey, 8-10 September 2011, pp. 825-830.

[18] L. Szabó, D. Fodorean, Simulation of the converter-machine assembly used used in electromechanical systems, U.T. Press Publishing House, Cluj, 2009 (in Romanian).

[19] I. Stepina, "Complex Equation for Electric Machines at Transient Conditions", Boston, ICEMA, 1990.

[20] I. Vlad, A. Campeanu, S. Enache, M.A. Enache, Study of direct-on-line starting of low power asynchronous motors, International Conference on Electromechanical and Power Systems (SIELMEN), Chisinau, Republica Moldova, 2017, pp.137-142,

[21] I. Vlad, A. Campeanu, S. Enache, Operation Characteristics of Low Power Asynchronous Motors Supplied by Static Converters, International Conference on Electrica land Power Engineering EPE 2016, pp.191-196. G.E. Subtirelu, M. Dobriveanu, M.A.Enache, and N. Boteanu, "Virtual Instrument for Study Dynamic Regime of Variable Reluctance Synchronous Motors", ICATE 2014, Craiova, OCT 23-25, 2014.

[22] ***http://g-line.chess.cornell.edu/G-lineStatus/G-lineManuals/PCI-Boards/Keithley-KPCI3101-Manual.pdf

[23] ***http://www.testequity.com/documents/pdf/keithley/KPCI-3101A-KPCI-3102A-KPCI-3103A-KPCI-3104A.pdf

[24] http://syscom.ro/pdf/LEM-traductoare-de-curent.pdf.